ISSN 1070-3632, Russian Journal of General Chemistry, 2007, Vol. 77, No. 6, pp. 1093–1099. © Pleiades Publishing, Ltd., 2007.
Original Russian Text © Yu.A. Gubarev, N.Sh. Lebedeva, V.P. Andreev, Ya.P. Nizhnik, A.I. V'yugin, 2007, published in Zhurnal Obshchei Khimii, 2007, Vol. 77, No. 6, pp. 1006–1013.

Thermooxidative Decomposition of Heterocyclic *N*-Oxides

Yu. A. Gubarev[a], N. Sh. Lebedeva[a], V. P. Andreev[b], Ya. P. Nizhnik[b], and A. I. V'yugin[a]

[a] *Institute of Solution Chemistry, ul. Akademicheskaya 1, Ivanovo, 153045 Russia*
e-mail: gua@isc-ras.ru
[b] *Petrozavodsk State University, Petrozavodsk, Karelia, Russia*

Received July 6, 2006

Abstract — Thermooxidative decomposition of pyridine *N*-oxide, 4-(4-dimethylaminostyryl)pyridine *N*-oxide, 4-(4-methoxystyryl)pyridine *N*-oxide, quinoline *N*-oxide, 2-methylquinoline *N*-oxide, 4-chloroquinoline *N*-oxide, 2-styrylquinoline *N*-oxide, and 2-(4-dimethylaminostyryl)quinoline *N*-oxide was studied. The kinetic parameters of the thermooxidative processes were calculated according to three independent procedures. The relation between the nature of heterocyclic *N*-oxide and its stability to thermal oxidation was analyzed.
DOI: 10.1134/S1070363207060254

Heterocyclic *N*-oxides are biologically active substances [1]. The spectrum of their activity is very broad: it extends from environmentally safe plant growth stimulants [2] and medical agents to exceptionally potent mutagens and cancerogens [3]. It is known that pyridine *N*-oxides are capable of losing oxygen on heating. Thermal deoxygenation occurs when *N*-oxides are heated in various solvents or without a solvent in the presence of solid catalysts. For example, pyridine *N*-oxide yields pyridine at 220°C; the reaction is accelerated in the presence of copper or zinc. 4-Ethoxypyridine *N*-oxide [4] and *N*-oxides of the quinoline series [5] behave similarly. The ability of *N*-oxides to readily lose oxygen was used to oxidize sulfoxides to sulfones [6], alkenes to epoxy derivatives [7], and carbenes [8, 9]. Some *N*-oxides (including triethylamine *N*-oxide and *N,N*-dimethylaniline *N*-oxide) were successfully synthesized by reversible oxygen transfer from pyridine and quinoline *N*-oxides to tertiary nitrogen atom on strong heating [10].

Thus heteroaromatic *N*-oxides can eliminate oxygen on heating and oxidize appropriate substrates. Studies on these processes are especially important taking into account that numerous derivatives of heterocyclic compounds are convenient to obtain via the corresponding *N*-oxides with subsequent deoxygenation. Insofar as many reactions performed at elevated temperature are accompanied by tarring and decomposition processes, leading to reduced yield of the target products, it is necessary to know thermal stability of *N*-oxides and the structure of possible thermooxidative decomposition products. In particular, deoxygenation is responsible in some cases for reduced yields of *N*-oxides in their syntheses [4].

There are published data [11–19] on the melting points and decomposition temperatures of *N*-oxides of the quinoline and pyridine series, as well as of their styryl derivatives. However, data on the pyrolysis and thermooxidative decomposition of these compounds and the corresponding kinetic parameters (activation energies E_a, orders of reaction n, preexponential factor A) are almost absent. Therefore, the goal of this study was to examine thermooxidative decomposition of pyridine *N*-oxide (**I**), 4-(4-dimethylaminostyryl)pyridine *N*-oxide (**IIa**), 4-(4-methoxystyryl)pyridine *N*-oxide (**IIb**), quinoline *N*-oxide (**IIIc**), 2-methylquinoline *N*-oxide (**IIId**), 4-chloroquinoline *N*-oxide (**IV**), 2-(4-dimethylaminostyryl)quinoline *N*- oxide (**Va**), and 2-styrylquinoline *N*-oxide (**Vc**) by thermogravimetry and determine the kinetic parameters of their thermal oxidation.

The thermal oxidation of compound **IIIc** includes several steps (Table 1). In the first step (294–407 K), crystal water molecules are removed. The weight loss at that step is about 22–22.6%, indicating the **IIIc**: H_2O ratio to be equal to 1 : 2 (1 : 2.24) (Fig. 1a). The two water molecules in the crystal hydrate **IIIb** $\cdot 2H_2O$ are thermodynamically nonequivalent, as follows from the presence of two peaks on the DTG curve (Fig. 1b) and the corresponding two peaks on the DTA curve (Fig. 1c). Elimination of the first water molecule from the crystal hydrate (**IIIc** $\cdot 2H_2O \rightarrow$ **IIIc** $\cdot H_2O$) involves

Table 1. Temperature ranges (K) of different steps of thermooxidative decomposition of heterocyclic *N*-oxides

Comp. no.	Step *I*	Step *II*	Step *III*	Step *IV*	Step *V*	Step *VI*
I	413–580	580–655	655–745	–	–	–
IIa	496–532	533–610	–	–	–	–
IIb	303–384	417–439	467–585	–	–	–
IIIc	294–407	407–460	460–500	500–573	–	–
IIId	292–362	362–397	397–481	481–687	687–798	–
IV	292–393	393–424	424–482	482–595	595–753	753–954
Va	305–457	457–597	–	–	–	–
Vc	293–463	463–531	532–623	623–725	730–871	–

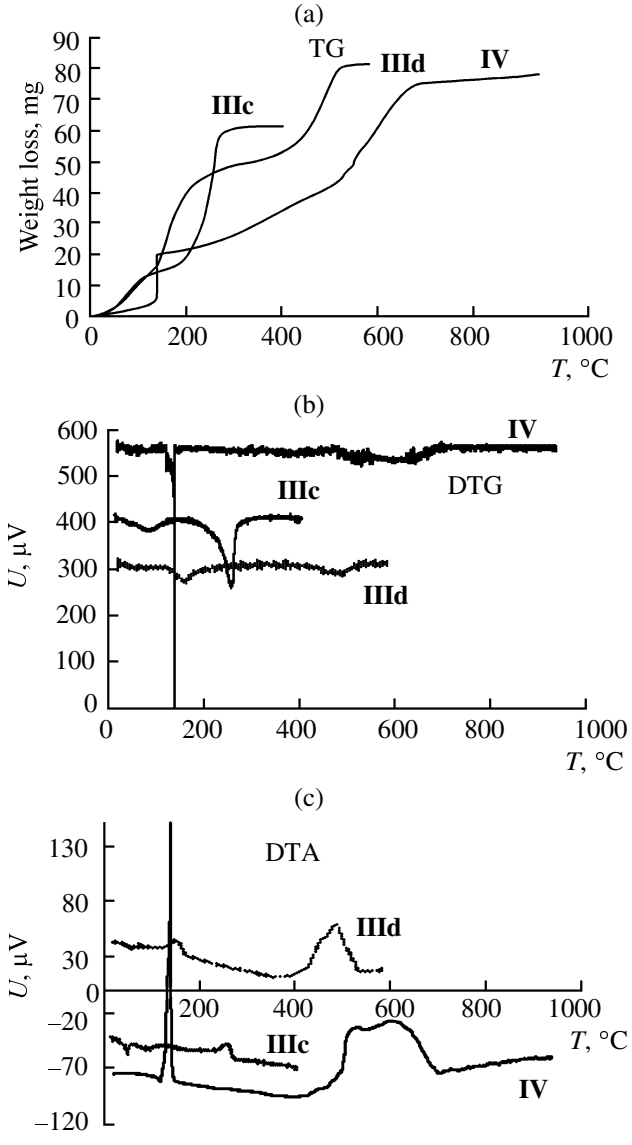

Fig. 1. Typical thermograms for the thermal oxidation of quinoline *N*-oxide (**IIIc**), 2-methylquinoline *N*-oxide (**IIId**), and 4-chloroquinoline *N*-oxide (**IV**): DTG is differential thermogravimetry, DTA is thermogravimetric analysis, and TG is thermogravimetry.

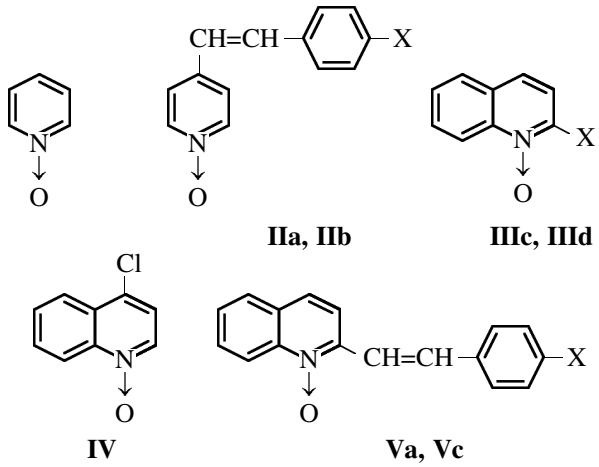

X = Me_2N (**a**), MeO (**b**), H (**c**), Me (**d**).

change in the enthalpy by 43.37 kJ mol^{-1}, and the DTA curve contains a relatively strong and sharp endothermic peak. Its shape suggests that the process is accompanied by melting of crystalline sample. These data are consistent with those reported in [14], where the melting point of **IIIc** · $2H_2O$ was estimated at 333 K. The complete dehydration (**IIIc** · $H_2O \rightarrow$ **IIIc**) is characterized by an enthalpy corresponding to vaporization of water (56.14 kJ mol^{-1}). The obtained $\Delta_{vap}H$ values roughly reflect the energy of intermolecular interaction between quinoline *N*-oxide and water and confirm energetical nonequivalence of the two water molecules in the crystal hydrate.

It is known that heterocyclic *N*-oxides are capable of interacting with two proton donors to give two possible structures [20]:

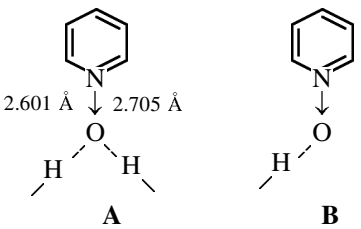

Table 2. Kinetic parameters of thermooxidative decomposition of heterocyclic *N*-oxides

Comp. no.	Step no.	Temperature, K	E_a, kJ mol^{-1}	ln(*A*)	Order of reaction, *n*	r^2	$F(\alpha)$	Model	Reference
I	*I*	413–580	96.06	–	–	0.997	–	–	[27]
			55.46	14.69	–	0.992	(1 – α)	F1	[28]
			42.03	–	1	0.982	–	–	[29]
	III	655–745	96.06	–	–	0.997	–	–	[27]
			67.86	18.31	–	0.968	(1 – α)	F1	[28]
			51.03	–	1	0.968	–	–	[29]
IIa	*I*	496–532	372.06	–	–	0.981	–	–	[27]
			232.28	56.13	–	0.942	(1 – α)	F1	[28]
			295.52	–	1	0.988	–	–	[29]
IIb	*II*	417–439	368.66	–	–	0.989	–	–	[27]
			213.96	62.52	–	0.932	(1 – α)	F1	[28]
			256.79	–	1	0.996	–	–	[29]
	III	467–585	139.38	–	–	0.984	–	–	[27]
			69.85	16.36	–	0.952	(1 – α)	F1	[28]
			74.32	–	1	0.988	–	–	[29]
IIIc	*III–IV*	460–673	142.20	–	–	0.997	–	–	[27]
			107.23	26.40	–	0.969	(1 – α)	F1	[28]
			109.63	–	1	0.978	–	–	[29]
IIId	*III*	397–481	134.15	–	–	0.991	–	–	[27]
			54.79	16.65	–	0.907	(1 – α)	F1	[28]
			70.77	–	1	0.987	–	–	[29]
IV	*II*	393–424	595.66	–	–	0.94	–	–	[27]
			255.12	78.16	–	0.775	(1 – α)	F1	[28]
			309.32	–	1	0.86	–	–	[29]
Va	*II*	457–597	53.27	–	–	0.964	–	–	[27]
			59.57	16.51	–	0.976	(1 – α)	F1	[28]
			58.66	–	1	0.980	–	–	[29]
Vc	*II*	463–531	423.53	–	–	0.985	–	–	[27]
			134.32	33.65	–	0.788	(1 – α)	F1	[28]
			157.04	–	1	0.954	–	–	[29]

Structure **A** was found in most cases [21], e.g., in tris[hydrogenbis(pyridine *N*-oxide)] hexathiocyanatochromate(III) [22] and 2,6-dimethylpyridine *N*-oxide–pentachlorophenol complex (1 : 2) [23]. Structure **B** was reliably identified in 4-dimethylaminopyridine *N*-oxide dihydrate [24] and 2,2'-bipyridine 1,1'-dioxide dihydrate [25]. The results of X-ray powder analysis of **IIIc**·$2H_2O$ [26] showed that two water molecules are involved in hydrogen bonding with the *N*-oxide oxygen atom. The length of one of these O···H bonds is 2.705 Å, and of the other, 2.601 Å (structure **A**). Thus the X-ray diffraction data also indicate nonequivalence of the water molecules in dihydrate **IIIc**·$2H_2O$.

The second step of the process (407–460 K) is characterized by monotonic change of all the recorded parameters and by insignificant weight loss (about 5.2%). When the temperature reaches 460 K, thermooxidative decomposition clearly starts. In the temperature range up to 500 K, the weight loss amounts to 16%, and a small exothermic peak is observed on the DTA curve (T_{max} = 490 K). The next step (500–573 K) is characterized by the maximal exothermic effect (T_{max} = 533 K) with a weight loss of 56.2%. These steps are indistinguishable on the DTG curve; therefore, the kinetic parameters were calculated for the temperature range 460–573 K (Tables 2, 3). The obtained data are well described in terms of the F1 model [28] (see Experimental); this implies that the rate-determining stage of thermal decomposition of quinoline *N*-oxide is diffusion [30].

Let us consider the results obtained for 4-chloroquinoline *N*-oxide (**IV**). The presence of chlorine strongly affects the thermal stability. The first step

Table 3. Average activation energies (kJ mol^{-1}) of steps *I*–*IV* in thermooxidative decomposition of heterocyclic *N*-oxides

Comp. no.	Step *I*	Step *II*	Step *III*	Step *IV*
I	48.74	–	59.44	–
IIa	263.90	–	–	–
IIb	–	235.38	72.09	–
IIIc	–	–	108.44	–
IIId	–	–	62.78	–
IV	–	282.2	–	–
Va	–	57.17	–	–
Vc	–	145.68	–	–

(292–393 K) is accompanied by a weight loss of about 4.8%, presumably due to partial sublimation. The absence of crystallization water in crystalline *N*-oxide **IV** (in contrast to **IIIc**) is consistent with the theoretical views. Electron-withdrawing chlorine atom reduced the electron density on the oxygen atom in the *N*-oxide moiety; therefore, proton-acceptor power of the oxygen atom and its ability to form H complexes become weaker.

In the second step (393–424 K) of thermooxidative decomposition of 4-chloroquinoline *N*-oxide the sample weight sharply decreases, and vigorous evolution of gaseous products is observed (a strong sharp peak on the DTG curve; Fig. 1b). Our results and published data led us to presume that this step includes elimination of halogen. The concentration of chlorine in **IV** is 19.74%, and the weight loss at the second step (with account taken of weight loss at the first step) is about 22.9%. The kinetic parameters calculated for the second step according to the Sestak–Berggren and Coats–Redfern procedures showed no consistency with each other (Table 2). The activation energy calculated from the data of differential termogravimetry differs by a factor of more than 2 from the E_a value determined according to Sestak–Berggren and Coats–Redfern. The reason for the observed disagreement is the high rate of removal of gaseous pyrolysis products, and the calculations cannot be performed with a required accuracy. It should be noted that the value E_a = 282.2 kJ mol^{-1} (calculated as an average of E_a values estimated according to Sestak–Berggren and Coats–Redfern) approaches the activation anergy of the process $C_2H_5Cl \rightarrow C_2H_4$ (E_a = 237.8 kJ mol^{-1}) [31]. As reported in [14], 4-chloroquinoline *N*-oxide melts at 406–408 K. Our results, specifically a considerable exothermic effect on the DTA curve (T_{max} = 408 K) did not allow us to interpret processes occurring at 393–424 K as melting of the sample of **IV**. Further raising the temperature gives rise to three more thermooxidative decomposition steps starting at 482, 595, and 753 K.

The pyrolysis of 2-methylquinoline *N*-oxide (**IIId**) also includes several steps. In the first step (292–362 K) no decomposition occurs, but crystallization water is removed; the weight loss (13.3%) corresponds to a crystal hdrate composition of 1 : 1. Pentimalli [16] reported on the **IIId** · 0.5 H_2O crystal hydrate with mp 350–351 K. According to our data, the monohydrate **IIId** · H_2O melts at 334 K. The next step (397–481 K) is accompanied by a weight loss of about 32% and a small exothermic peak on the DTA curve (Figs. 1a, 1c). The kinetic parameters of the thermal oxidation process are given in Tables 2 and 3. It is seen that introduction of a methyl group into the 2-position of the quinoline ring reduces the activation energy and decomposition temperature.

Typical derivatograms of styryl-substituted quinoline *N*-oxides are shown in Fig. 2. As follows from the data in Fig. 2 and Table 1, 2-styrylquinoline *N*-oxide (**Vc**) is the most thermally stable among the examined quinoline *N*-oxides. The first step (293–463 K) is likely to involve sublimation, melting, and evaporation of the sample. Its melting corresponds to a relatively strong endothermic peak on the DTA curve (393 K). According to [32], compound **Vc** melts at 389–391 K. The next step (463–531 K) is accompanied by a weight loss of about 16%, and an exothermic peak appears on the DTA curve.

The kinetic parameters of the initial step of thermooxidative decomposition of *N*-oxide **Vc** (Tables 2, 3; step *II*) considerably exceed those found for compound **IIIc**; presumably, *N*-oxide **Vc** is stabilized due to conjugation with the styryl substituent. At higher temperatures, three more thermal decomposition steps starting at 532, 623, and 730 K are observed.

Likewise, 2-(4-dimethylaminostyryl)quinoline *N*-oxide (**Va**) decomposes in several steps. It undergoes sublimation at relatively low temperatures (up to 457 K), and no melting of a sample of **Va** is observed on the DTA curve. Thermooxidative decomposition begins at 457 K and is accompanied by exothermic peak on the DTA curve.

Apart from *N*-oxides of the quinoline series, we examined thermooxidative decomposition of pyridine *N*-oxide (I), 4-(4-dimethylaminostyryl)pyridine *N*-oxide (**IIa**), and 4-(4-methoxystyryl)piridine *N*-oxide (**IIb**). The corresponding derivatograms are shown in Fig. 3, and the kinetic parameters of the initial thermal

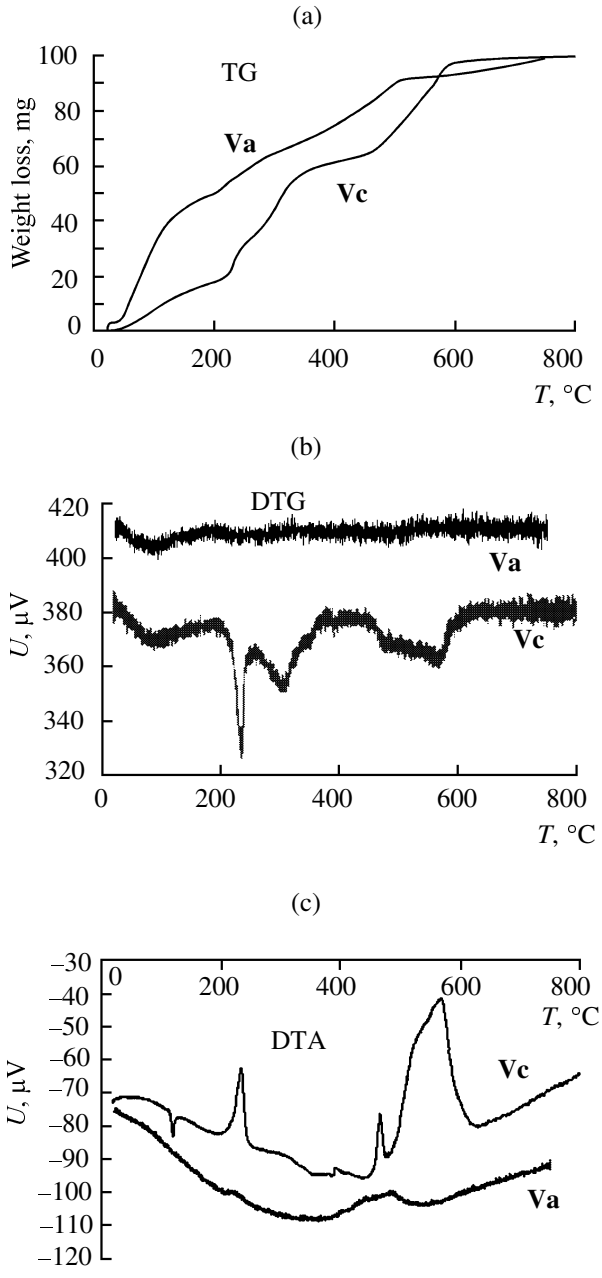

Fig. 2. Typical derivatograms of 2-styrylquinoline *N*-oxides **Va** and **Vc**. For designation of curves, see legend to Fig. 1.

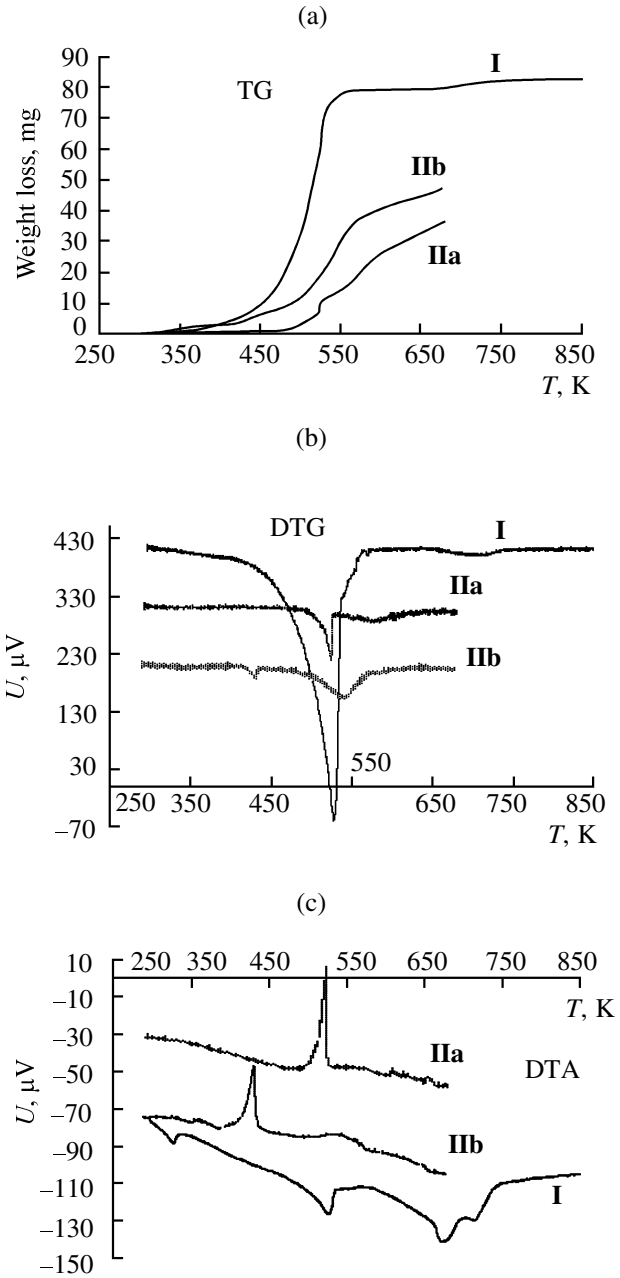

Fig. 3. Typical derivatograms of 4-styrylpyridine *N*-oxides **IIa** and **IIb**. For designation of curves, see legend to Fig. 1.

oxidation step are given in Tables 1–3. Obviously, styryl substituents containing amino and methoxy groups considerably affect the stability of heterocyclic *N*-oxides to thermooxidative decomposition: increased basicity of these compounds due to donor character of the substituents (see below) makes them more thermally stable.

The thermal stability of the examined *N*-oxides of the quinoline and pyridine series, estimated by the temperature at which their decomposition starts, increases in the following series: (1) **IV** < **IIId** << **Va** ≤ **IIIc** < **Vc** and (2) **I** ≤ **IIb** < **IIa**. The energy of activation of the first thermooxidative decomposition step increases in the series (3) and (4): (3) **Va** < **IIId** < **IIIc** < **Vc** < **IV**; (4) **I** < **IIb** < **IIa**. It is seen that series (1) and (3) coincide except for the positions of **IV** and **Va**. This may be due to different mechanisms of thermooxidative decomposition of quinoline *N*-oxides **IV** and **Va**. Probably, the first step of the process

involves different reaction centers in these compounds. For example (see above), the first step of decomposition of *N*-oxide **IV** is its dehalogenation.

It should be noted that electron-withdrawing substituents reduce the thermal stability of *N*-oxides; this is consistent with published data: prolonged heating (463–473 K, 10 h) of nicotinic acid *N*-oxide with pyridine leads to quantitative transformation of the latter into pyridine *N*-oxide with simultaneous deoxygenation of nicotinic acid *N*-oxide [33].

The pyridine *N*-oxide series (2) and (4) coincide, indicating similar mechanisms of their thermal oxidation at the given step. Series (2) and (4) show a relation with the Hammett constants σ:

N-Oxide	**IIa**	**IIb**	**I**
$\sigma_{N\text{-oxide}}$ [34]	–0.31	–0.22	0
σ [34]	–0.15	–0.05	0

The revealed relations suggest a considerable role of the conjugation effect which is most pronounced for *para*-substituted pyridine *N*-oxides.

Thus, the results of our thermochemical study showed that the kinetic parameters of thermal oxidation of *N*-oxides strongly depend on the nature and position of substituent in their molecules and that the substituent effect not only extends to the reaction center but in some cases changes the mechanism of pyrolysis. Further studies are necessary to rationalize the revealed specificities of thermal decomposition of different *N*-oxides and identify products at different decomposition steps.

EXPERIMENTAL

All the examined heterocyclic *N*-oxides were synthesized and purified according to the procedures reported in [14, 18, 19].

Termochemical studies were performed on a thermoanalytical setup whose metrological and certification parameters were described in detail in [34]. Experiments were performed on exposure to air; heating rate 5 deg min^{-1}.

Mathematical processing of the results. All possible approaches to calculation of kinetic parameters of a reaction are based on the Arrhenius equation. We calculated the kinetic parameters according to the procedure described in [27], as well as using the Coats–Redfern [29] and Sestak–Berggren methods [28]. A mixture of $KMnO_4$ with Al_2O_3 was used as reference substance to estimate the validity of the calculated kinetic parameters. The activation energy for the reference system was estimated at 140.52 ± 1.00 kJ mol^{-1} (correlation coefficient no less than 0.961), which is well consistent with published data [27] recommended for that system.

Specificities of intermolecular interactions of heterocyclic *N*-oxides with crystallization water were also studied by thermogravimetric analysis; this method makes it possible to determine the composition of crystal hydrates, change in the enthalpy during vaporization of solvent molecules from solvates, and decomposition temperature. The detailed procedure for the determination of the above physical parameters was described in [34, 35].

REFERENCES

1. Albini, A. and Pietra, S., *Heterocyclic N-Oxides,* Boca Raton: CRC, 1991, p. 312.
2. Ponomarenko, S.P., *Regulyatori rostu roslin u zemlerobstvi. Zbirnik naukovikh prats* (Plant Growth Regulators in Agriculture. A Collection of Scientific Papers), Shevchenko, A.O., Ed., Kiev: Agroresursi, 1998.
3. Fukuhara, K., Hakura, A., Sera, N., Tokiwa, H., and Miyata, N., *Chem. Res. Toxicol.,* 1992, vol. 5, no. 2, p. 149.
4. Katritzky, A.R. and Lagowski, J.M., *Chemistry of the Heterocyclic N-Oxides,* London: Academic, 1971.
5. Kosige, T., Adachi, K., Yokota, M., and Nakao, T., *J. Pharm. Soc. Jpn.,* 1965, vol. 85, no. 1, p. 66.
6. Biffin, M.E.C., Boeksteiner, G., Miller, J., and Paul, D.B., *Aust. J. Chem.,* 1974, vol. 27, no. 4, p. 789.
7. Strub, H., Strehler, C., and Streith, J., *Chem. Ber.,* 1987, vol. 120, no. 3, p. 355.
8. Schweizer, E., O'Neill, G., and Wemple, J., *J. Org. Chem.,* 1964, vol. 29, no. 5, p. 1744.
9. D'yakonov, I.A., Mandel'shtam, T.V., and Radul, O.M., *Zh. Org. Khim.,* 1968, vol. 4, no. 4, p. 723.
10. Ryzhakov, A.V. and Rodina, L.L., *Sintez, stroenie i khimicheskie prevrashcheniya organicheskikh soedinenii azota: nitrosoedinenii, aminov i aminokislot* (Synthesis, Structure, and Chemical Transformations of Organic Nitrogen Compounds: Nitro Compounds, Amines, and Amino Acids), Leningrad: 1991, p. 11.
11. Marinho, E.P., Borges, F.M.M., Araujo Melo, D.M., Scatena, H., Jr., Zinner, L.B., and Zinner, K., *Thermochim. Acta,* 2000, vol. 344, p. 81.
12. Dunstan, P.O., *Thermochim. Acta,* 2004, vol. 409, p. 19.
13. Vrbova, M., Baran, P., Boca, R., Fuess, H., Svoboda, I., Linert, W., Schubert, U., and Wiede, P., *Thermochim. Acta,* 2000, vol. 19, p. 2195.

14. Ochiai, E.R., *J. Org. Chem.,* 1953, vol. 18, p. 534.
15. *Svoistva organicheskikh soedinenii. Spravochnik* (Properties of Organic Compounds. A Reference Book), Potekhin, A.A., Ed., Leningrad: Khimiya, 1984.
16. Pentimalli, L., *Gazz. Chim. Ital.,* 1963, vol. 93, p. 1093.
17. Brink, C.v.d.M. and de Jager, P.J., *Tydskr. Natuurwet.,* 1963, vol. 3, no. 2, p. 74; *Ref. Zh., Khim.,* 1964, no. 10Zh226.
18. Andreev, V.P., Ryzhakov, A.V., and Tekanova, S.V., *Khim. Geterotsikl. Soedin.,* 1995, no. 4, p. 518.
19. Titskii, G.D. and Turovskaya, M.K., *Zh. Org. Khim.,* 1992, vol. 28, no. 9, p. 1911.
20. Prezhdo, V.V., Vashenko, E.V., Prezhdo, O.V., and Pushko, A., *J. Mol. Struct.,* 1999, vol. 510, p. 69.
21. Allen, F.H., *Acta Crystallogr., Sect. B.,* 2002, vol. 58, p. 380.
22. Cherkasova, T.G. and Mezentsev, K.V., *Russ. Coord. Chem.,* 2002, vol. 28, p. 510.
23. Dega-Szafran, Z., Kosturkiewicz, Z., Tykarska, E., Szafran, M., Lemanski, D., and Nogaj, B., *J. Mol. Struct.,* 1997, vol. 404, p. 25.
24. Nakai, H., Saito, T., and Yamakawa, M., *Acta Crystallogr., Sect. C,* 1988, vol. 44, p. 533.
25. Ye, M.-D., Hu, M.-L., Yuan, J.-X., and Wang, S., *Z. Crystallogr., New Cryst. Struct.,* 2002, vol. 217, p. 497.
26. Ivashevskaja, S.N., Aleshina, L.A., Andreev, V.P., Nizhnik, Y.P., and Chernyshev, V.V., *Acta Crystallogr., Sect. E,* 2002, vol. 58, p. 920.
27. Zatsepin, A.F. and Fotiev, A.A., *Zh. Neorg. Khim.,* 1973, vol. 18, no. 11, p. 2883.
28. Sestak, J. and Berggren, G., *Thermochim. Acta,* 1972, vol. 3, p. 498.
29. Coats, A.W. and Redfern, J.P., *Nature,* 1964, vol. 201, p. 68.
30. Segal, E., *Festkorperchemie,* Boldyrev, V.V. and Meyer, K., Eds., Leipzig: Grundstoffindustrie, 1973, p. 404.
31. Gordon, A.J. and Ford, R.A., *The Chemist's Companion,* New York: Wiley, 1972.
32. Andreev, V.P., Nizhnik, Ya.P., Bezruchko, D.G., and Morozov, A.K., *Russ. J. Gen. Chem.,* 2005, vol. 75, no. 8, p. 1309.
33. Ryzhakov, A.V. and Elaev, N.R., *Khim. Geterotsikl. Soedin.,* 1987, no. 8, p. 1075.
34. Lebedeva, N.Sh., Yakubov, S.P., Kinchin, A.N., and V'yugin, A.I., *Zh. Fiz. Khim.,* 2005, vol. 79, no. 5, p. 955.
35. Suvorov, A.V., *Termodinamicheskaya khimiya paroobraznogo sostoyaniya* (Thermodynamics and Chemistry of the Gaseous State), Leningrad: Khimiya, 1970, p. 208.